

# Scaling the saturated hydraulic conductivity of an alfisol

M. BONSU & K. B. LARYEA

*International Crops Research Institute for the Semi-Arid Tropics, Patancheru P.O.,  
Andhra Pradesh 502 324, India*

## SUMMARY

Alfisols exhibit a high degree of spatial variability in their physical properties. As a result, it is difficult to use information on physical parameters measured at one location to model larger-scale hydrologic processes. In this study, the saturated hydraulic conductivity,  $K_s$ , of an Alfisol was determined on 109 undisturbed monoliths using the falling-head permeameter method. The model developed by Arya & Paris (1981) was used to calculate the pore volume from sand and clay fractions. Scaling factors were calculated from the measured  $K_s$ , sand pore-volume, clay pore-volume, clay content and effective porosity, using the similar media concept. Prediction of  $K_s$  of gravelly Alfisol using clay pore-volume is confounded by high gravel content which, when discounted, improves the prediction remarkably. The scaled mean saturated hydraulic conductivity  $K^*$  for all horizons of the Alfisol was approximately  $1.0 \times 10^{-5} \text{ m s}^{-1}$ .

## INTRODUCTION

Alfisols occupy about 30% of the land area in the semi-arid tropics (SAT), but their low water-holding capacity owing to their characteristically shallow depth is one of the major constraints to sustained crop production (El-Swaify *et al.*, 1987). There is little available information on their hydraulic properties. The low water-holding capacity of the SAT Alfisols may be, in part, attributed to the fact that little water is transmitted to deeper layers of the profile. Therefore, a knowledge of the hydraulic properties is essential for *in situ* water management of these soils.

Alfisols exhibit a high degree of spatial variability, both in their texture and structure. The variability in soil structural and textural attributes is also manifest in the non-uniformity of the horizon depths. Consequently, replicate determinations of soil physical and chemical parameters over short distances are often so variable as to make rational use difficult.

One way to address the problem of variability is by using scaling factors. As noted by Tillotson & Nielsen (1984), scaling factors are simple conversion factors relating characteristics of one system to corresponding characteristics of another. These are best derived from a knowledge of the physical quantities known to govern specific processes through dimensional techniques. Scaling factors may also be derived through regression analysis—a technique called functional normalization (Tillotson & Nielsen, 1984). The purpose of scaling (or using scaling factors) is to coalesce information of a spatially-variable property into a unified representation. This assists mathematical modelling. Since the introduction of scaling factors in the concept of similar media (Miller & Miller, 1956), considerable effort has been devoted to scaling unsaturated flow of water in soils (Warrick *et al.*, 1977; Simmons *et al.*, 1979; Jury *et al.*, 1987; Youngs, 1987).

Saturated hydraulic conductivity,  $K_s$ , has many important implications in irrigation and drainage systems design (Bouwer & Jackson, 1974), infiltration and general water-balance modelling (Hachum & Alfaro, 1977; Chong & Green, 1979; Ahuja *et al.*, 1984b). Field methods for determining saturated hydraulic conductivity are tedious, time-consuming, expensive and require

training. Consequently, information on the saturated hydraulic conductivity of Alfisols in the SAT is scarce. Therefore, scaling hydraulic conductivity using scaling factors calculated from easily measured soil properties like particle size will have some advantages.

This study compares the frequency distribution of scaling factors obtained from measured  $K_s$  with those from effective porosity (Ahuja *et al.*, 1984a) as well as particle size or pore volume associated with particle size (Arya & Paris, 1981), in order to ascertain if the scaling factors from these easily measured soil properties can be used to scale saturated hydraulic conductivity of a field soil.

### THEORETICAL

Following Warrick *et al.* (1977) and Simmons *et al.* (1979) we characterize the areal variability of  $K_s$  in terms of scaling factors used in the Miller & Miller (1956) treatment of similar media as

$$K_{si} = \alpha_i^2 K^* \quad (1)$$

In Equation (1),  $K_{si}$  is the saturated hydraulic conductivity of a certain soil horizon at a given location  $i$ ,  $K^*$  is the scaled mean saturated hydraulic conductivity for all horizons, and  $\alpha_i$  is a scaling factor for location  $i$ . By setting the mean of  $\alpha_i$  values to 1.0, Equation (1) can be rewritten to obtain  $K^*$  from a sample size of  $n$  measurements of  $K_{si}$  (Warrick *et al.*, 1977; Jury *et al.*, 1987) as

$$K^* = \left[ \frac{1}{n} \sum_{i=1}^n (K_{si})^{\frac{1}{2}} \right]^2 \quad (2)$$

We now define a relationship such that either  $K_s$  is a function of the effective porosity  $\phi_{ei}$

$$K_{si} = f(\phi_{ei}); \quad (3a)$$

or that  $K_s$  is a function of the pore volume  $V_{pi}$

$$K_{si} = f(V_{pi}). \quad (3b)$$

In more detail,  $\phi_{ei}$  is defined as the total porosity minus soil water content at  $-33$  kPa pressure potential (Ahuja *et al.*, 1984a), whereas  $V_{pi}$  is the particle size, or the pore volume associated with the sand or clay particle size at location  $i$ . Combining Equation (1) with Equations (2), (3a) and (3b) gives three scaling factors  $\alpha_{ij}$  thus:

$$\alpha_{i1} = n(K_s) / \sum_{i=1}^n (K_{si})^{\frac{1}{2}}, \quad (4a)$$

$$\alpha_{i2} = n[f(\phi_{ei})]^{\frac{1}{2}} / \sum_{i=1}^n [f(\phi_{ei})]^{\frac{1}{2}}, \quad (4b)$$

$$\alpha_{i3} = n[f(V_{pi})]^{\frac{1}{2}} / \sum_{i=1}^n [f(V_{pi})]^{\frac{1}{2}}. \quad (4c)$$

Our approach here is to compare, firstly, the frequency distributions of  $\alpha_{i1}$  from Equation (4a) with the distributions of  $\alpha_{i2}$  and  $\alpha_{i3}$  from Equations (4b) and (4c). If the frequency distribution of  $\alpha_{i1}$  is similar to that of  $\alpha_{i2}$  or  $\alpha_{i3}$ , then for a given  $K^*$  we can use either the  $\alpha_{i2}$  or  $\alpha_{i3}$  distribution to calculate  $K_{si}$  of a similar site from Equation (1).

#### Expressing porosity of gravelly soils

Because Alfisols at the International Crops Research Institute for the Semi-Arid Tropics (ICRISAT) Centre are characteristically gravelly, we account for the effect of gravel on the total porosity ( $f$ ) by considering the basic definition,

$$f = V_f / V_t \quad (5)$$

where  $V_f$  is the volume of pores, and  $V_t$  is the bulk volume of soil, including gravel. Equation (5) may be rewritten as

$$f = (V_t - V_{sg}) / V_t \quad (6)$$

where  $V_{sg}$  is the sum of the volume of fine soil  $V_s$ , and that of gravel  $V_g$ . Replacing  $V_{sg}$  in Equation (6) with  $(V_s + V_g)$  and expressing the volume ( $V$ ) in terms of mass ( $M$ ) and density ( $D$ ), it can be shown that

$$f = 1 - [(M_s/M_t)(D_b/D_s) + (M_r/M_t)(D_b/D_r)] \quad (7)$$

where  $M_s$  is the mass of fine soil,  $M_t$  is the total mass of soil plus gravel,  $M_r$  is the mass of gravel,  $D_r$  is the particle density of the gravel,  $D_b$  is the bulk density of the soil and  $D_s$  is the particle density of the soil. The effective porosity  $\phi_{ei}$  in Equation (4b) was obtained by subtracting the volumetric water content at  $-33$  kPa from the total porosity calculated with Equation (7).

#### Modelling pore volume from particle size

The model presented by Arya & Paris (1981) was adopted here to estimate the pore volume associated with a given particle size. If  $X$  is the ratio of the mass of a particular particle size to the mass of fine soil, then the mass  $P$  of the particular particle size in the sample is

$$P = XM_s(1 - R_w) \quad (8)$$

where  $R_w$  is the ratio of the mass of gravel to the total mass of the sample, including gravel. Assuming that the bulk density of the constituent particles does not differ significantly from the bulk density of the fine soil fraction, then the pore volume ( $V_p$ ) due to this particle size is

$$V_p = (P/D_t) - (P/D_s) \quad (9)$$

where  $D_t$  is what the bulk density of the field soil ( $<2$  mm) would be if the gravel were not present and defined as (Ravina & Magier, 1984)

$$D_t = D_b D_r (1 - R_w) / (D_r - R_w D_b) \quad (10)$$

Equation (9) can be written as

$$V_p = Pe/D_s \quad (11)$$

where the void ratio  $e$  is defined as

$$e = (D_s/D_t) - 1 \quad (12)$$

If  $V_p$  calculated from Equation (11) is functionally related to  $K_s$ , we can use Equations (11) and (4c) to obtain a distribution of scaling factors for  $K_s$ .

## MATERIALS AND METHODS

This study was carried out on 0.17 ha of a shallow Alfisol (Udic Rhodustalf) at ICRISAT Centre. The area was divided into nine plots 17 m by 11 m, with three plots in a row. A total of nine profiles was used.

#### Monolith excavation and preparation

A procedure similar to that reported by Bouma *et al.* (1976) was used to obtain soil monoliths for the determination of  $K_s$ . A pit was dug in each plot, and for each horizon undisturbed monoliths were carved *in situ*. Replicate cores obtained from the monoliths were 0.22 m in diameter and 0.15 m long, with the exception of the Ap horizon, where they were less than 0.15 m long. After carving, the outside of each core was plastered with quick-setting cement. The cores were fixed in PVC cylinders of 0.24 m diameter and 0.30 m long using a slurry of the quick-setting cement. Pre-plastering the cores prevented the cement slurry from entering the large pores. The slurry was allowed to solidify in the field. Because of shrinkage, more cement slurry was added until the level of the cement after solidifying was the same as the soil surface. The whole process took 1 day. The cores were removed, the bottom trimmed, and brought to the laboratory.

*K<sub>s</sub> determination*

The cores were slowly wetted from the bottom in large basins until the water level in the basins was approximately half way up the cores. The saturated hydraulic conductivity measurements were made using the falling-head permeameter method. A rectangular metal box, 0.88 m long, 0.58 m wide and 0.15 m deep, with two drainage outlets, was filled with gravel. The cores were supported on plastic sieves placed on gravel so that the matric potential at the base of the cores was zero before water moved out. The initial hydraulic head  $H_1$  and the fall of the hydraulic head on the soil surface as a function of time  $H_t$  was measured using a water manometer. A regression of  $\ln(H_1/H_t)$  on time ( $t$ ) and Equation (13) were used to calculate  $K_s$ . Thus,

$$K_s = bLA/a. \quad (13)$$

In Equation (13),  $b$  is the slope of the regression of  $\ln(H_1/H_t)$  on  $t$ ,  $L$  is the length of the sample,  $A$  is the area of the PVC cylinder, and  $a$  is the surface area of the soil sample. Generally, the coefficient of determination for the  $\ln(H_1/H_t)$  vs  $t$  relationship was highly significant ( $r^2 > 0.99$ ).

*Determination of bulk density, particle density, and particle size*

The overall bulk density,  $D_b$ , of any core was calculated from the wet mass of the core and its gravimetric water content.

The soil from each core was then air-dried and passed through a 2 mm sieve. After sieving, the gravel was washed and oven dried. The bulk density of fine soil,  $D_p$ , was then calculated using Equation (10).

The soil particle density,  $D_s$ , was determined using kerosene displacement from pycnometer bottles. The particle size distribution was determined by the conventional hydrometer method after dispersion in sodium hexametaphosphate.

*Determination of effective porosity from total porosity and water content at -33 kPa*

The total porosity of samples used for the  $K_s$  determination was calculated by Equation (7). The water content at -33 kPa was determined on separate cores. With the exception of the gravelly horizons where the cores measured 50 mm in diameter and 30 mm in length, all cores were 50 mm in diameter and 10 mm in length. In taking the 10 mm long cores, three small cylinders were placed on top of each other and the whole assemblage was pressed down into the moist soil. The cores at the centre were used for the determination of water content at -33 kPa. In the gravelly horizons, two cylinders were placed on top of each other, a wooden plank was placed on the top cylinder, and the cores were taken by gently hammering the plank. The cores obtained in the bottom cylinders were wetted in the laboratory using the pressure-plate apparatus and the water content at -33 kPa determined. The porous plates were covered with a thin layer of slurry to ensure good soil-plate contact. The effective porosity was calculated as the difference between the total porosity and volumetric water content at -33 kPa (Ahuja *et al.*, 1984a).

## RESULTS AND DISCUSSION

*Physical characteristics*

The sand (2–0.02 mm), silt (0.02–0.002 mm), and clay (<0.002 mm) contents of the fine-soil fraction are plotted as a function of depth for four soil profiles in Fig. 1. The texture of the A horizons varied from loamy sand to sandy loam. Except for one sandy clay loam, the texture of the subsoils was either sandy clay or clay.

From all nine profiles, the plots of coarse fragments, particle density, overall bulk density and bulk density of the fine soil, as a function of depth, are presented in Fig. 2. The particle density and the bulk density of fine soil were low but the overall bulk density was high in the gravelly horizons. The large variation in particle density precludes using  $2.65 \text{ Mg m}^{-3}$  as an average particle density for this Alfisol. Similar low particle densities for a similar Alfisol at the ICRISAT Centre were reported by El-Swaify *et al.* (1987). The total porosity was usually low in the gravelly horizons.

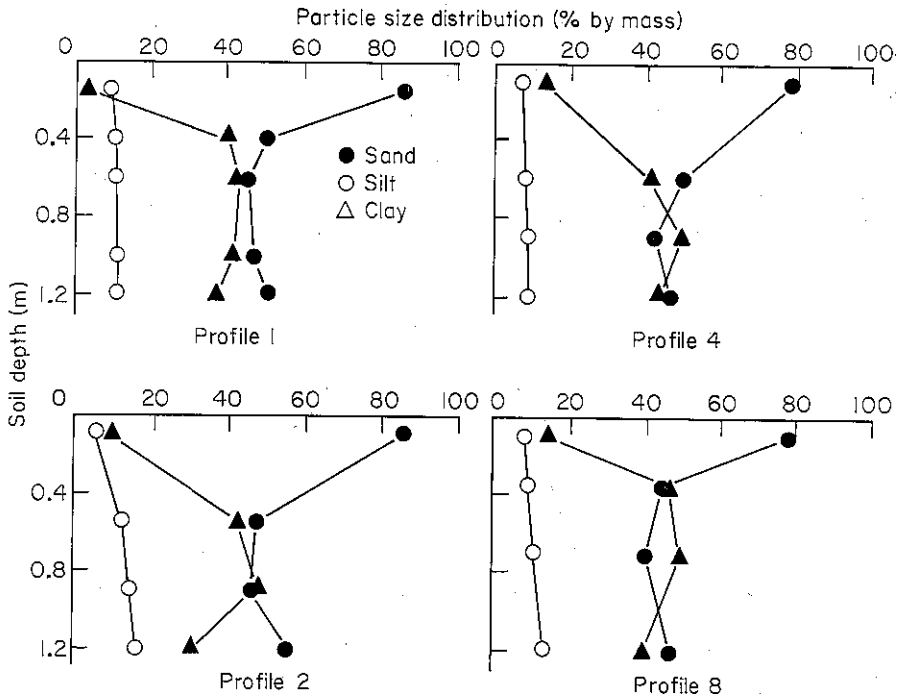


Fig. 1. Particle size distribution profiles of four profiles of the Alfisol.

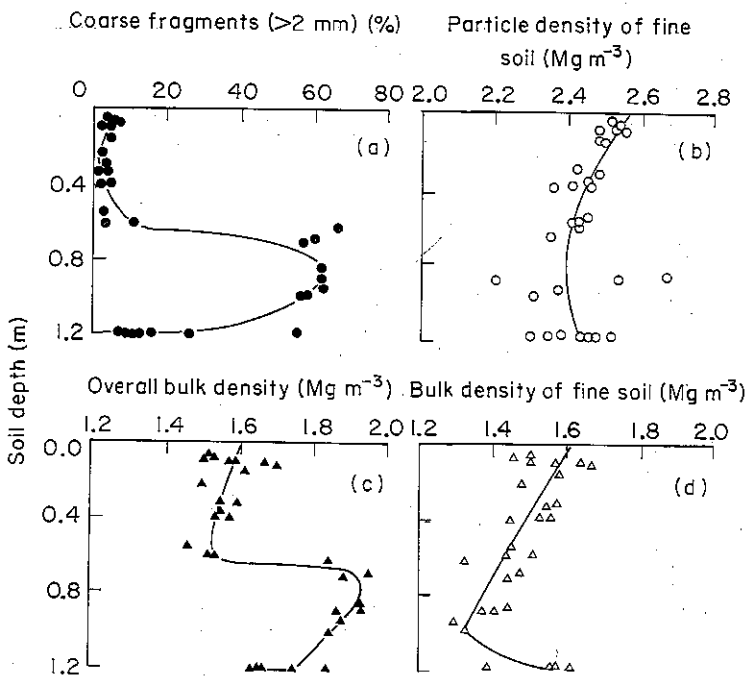


Fig. 2. Plots of coarse fragments (a), particle density (b), overall bulk density (c), and bulk density of fine soil (d) as a function of depth for the nine profiles.

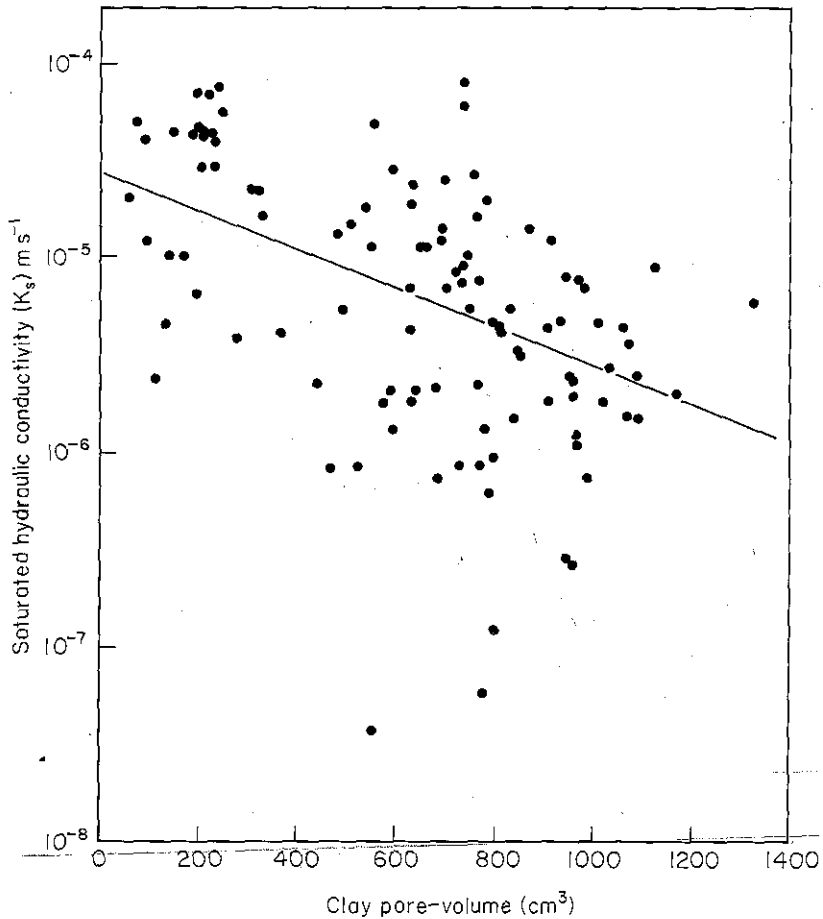


Fig. 3. Semi-log plot of  $K_s$  against clay pore-volume for the 109 samples.

#### Relating $K_s$ to physical properties

In order to select the important soil physical properties for scaling  $K_s$  by functional normalization technique (Tillotson & Nielsen, 1984) we carried out least-squares regression to relate  $K_s$  to clay content, as well as sand content, clay pore-volume, sand pore-volume, and effective porosity as the independent variables. Because semi-log transformed data gave the highest correlation coefficients, an exponential function was used to describe the relationship between  $K_s$  and the independent variables. In the analysis, we considered only those functional relationships which were significant at a probability level of 0.01 or less.

The regression of  $\ln K_s$  on clay content as well as on sand content was highly significant ( $r = -0.52$ ,  $P < 0.001$  for clay content;  $r = 0.47$ ,  $P < 0.001$  for sand content). However, we were unable to fit least-square lines through the data points relating  $\ln K_s$  to clay or sand content because the distribution of the data indicated a group of two populations with a pronounced vertical orientation. The regressions suggest an artifact of two populations with different means. A similar vertical clustering (of three populations) was reported by Puckett *et al.* (1984) for an exponential  $K_s$ -clay content relation in accordance with three textural classes present.

Since pore size distribution rather than soil texture *per se* physically determines  $K_s$  (Childs & Collis-George, 1950; Marshall, 1958), we expressed the clay and sand fractions in pore volumes using Equations (9) and (14). The silt fraction was omitted because the correlation between  $K_s$  and silt content was not significant.

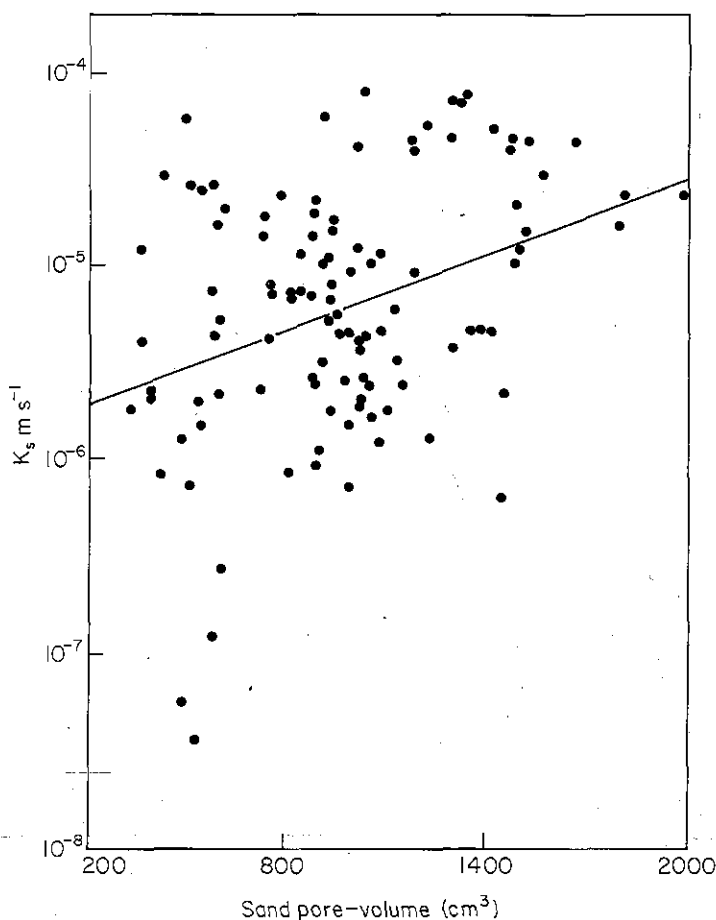


Fig. 4. Semi-log plot of  $K_s$  against sand pore-volume for the 109 samples.

The semi-logarithmic plot of  $K_s$  vs clay pore volume ( $C_v$ ) is shown in Fig. 3. The conversion of clay content to clay pore-volume eliminated the two textural groups resulting from  $\ln K_s$  vs clay content relation. Fig. 3 indicates that  $K_s$  decreased as  $C_v$  increased suggesting a decrease in water transmission pores as clay content increases.

The semi-logarithmic plot of  $K_s$  vs sand pore-volume ( $S_v$ ) is presented in Fig. 4. Like clay pore volume, the conversion of sand content to sand pore-volume eliminated the two textural groups that characterized  $\ln K_s$  and sand content relation. Fig. 4 indicates that  $K_s$  increased with an increase in  $S_v$ , probably owing to an increase of water transmission pores and increased pore continuity associated with increasing sand pore-volume.

The semi-log plot of  $K_s$  against effective porosity ( $\phi_e$ ) is illustrated in Fig. 5, which demonstrates that  $K_s$  increased with an increase of  $\phi_e$  which designates soil macroporosity (Ahuja *et al.*, 1984a).

The distribution of the gravel might influence the scatter in the  $K_s$  data. To investigate the influence of gravel on the variability of the  $K_s$ , we arbitrarily classified the samples as 'gravelly' whenever the gravel content was greater than 10%, and 'non-gravelly' whenever the gravel content was less than 10%. Table 1 shows the regression parameters of  $\ln K_s$  on the various soil physical properties for the non-gravelly samples. The absolute magnitude of the correlation coefficients increased with respect to clay content, clay pore-volume, sand content and sand pore-volume. Table 1 suggests that gravel content contributes in part to the variability in  $K_s$  of the Alfisol.

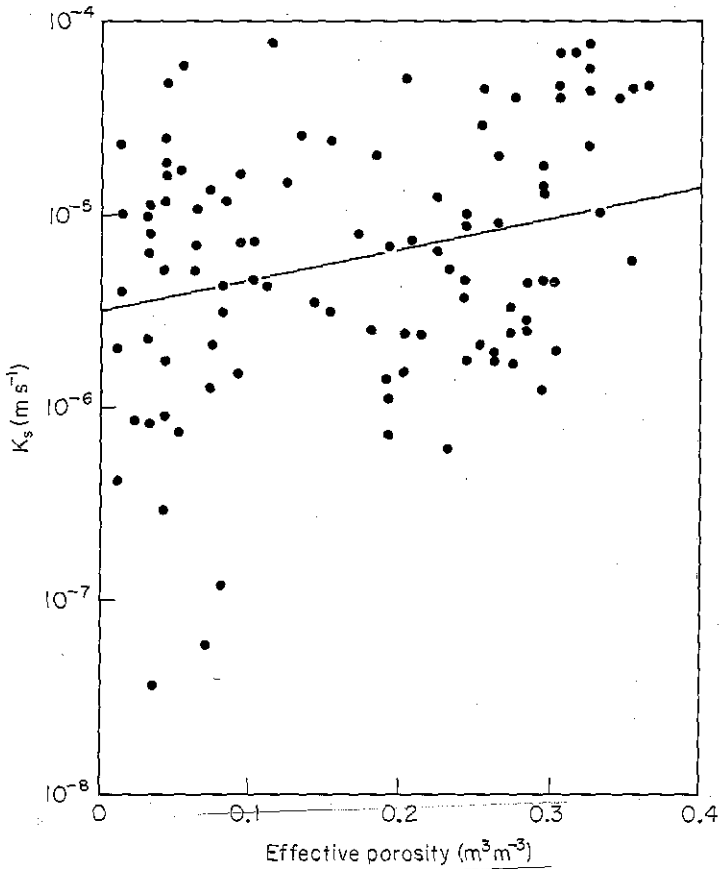


Fig. 5. Semi-log plot of  $K_s$  against effective porosity for the 109 samples.

Table 1. Regression parameters of  $\ln K_s$  on some soil physical properties for samples with <10% gravel content ( $n=68$ )

Variable	Intercept	Slope	$r$
$\ln K_s$ vs clay pore-volume	-10.42	-0.0024	-0.68***
$\ln K_s$ vs clay content	-10.23	-0.0550	-0.68***
$\ln K_s$ vs sand pore-volume	-14.10	0.0020	0.44***
$\ln K_s$ vs sand content	-14.66	0.0460	0.65***
$\ln K_s$ vs effective porosity	-12.70	3.7100	0.25*

\*\*\*Significant at  $P < 0.001$ . \*Significant at  $P < 0.05$ .

A major limitation of using Equation (9) to compute pore volume from particle size is the assumption that the bulk density of the textural component in question is the same as the bulk density of the fine soil. For the samples used, the highest sand content was 86% with a corresponding fine soil bulk density of  $1.6 \text{ Mg m}^{-3}$ , and the highest clay content was 53% with a corresponding fine soil bulk density of  $1.3 \text{ Mg m}^{-3}$ . These bulk densities were used in Equation (9) to compute the pore volume of sand and clay respectively. Table 2 shows the regression parameters of  $\ln K_s$  on clay



**Table 2.** Regression parameters of  $\ln K_s$  on sand pore-volume and clay pore-volume calculated with Equation (14) using bulk density of  $1.6 \text{ Mg m}^{-3}$  for sand and  $1.3 \text{ Mg m}^{-3}$  for clay ( $n=109$ )

Variable	Intercept	Slope	$r$
$\ln K_s$ vs clay pore-volume	-10.69	-0.0015	-0.43***
$\ln K_s$ vs sand pore-volume	-13.14	0.0014	0.33***

**Table 3.** Mean scaling factor  $a$ , standard deviation (SD) of  $a$ , and scaled mean saturated hydraulic conductivity,  $K^*$  of measured  $K_s$ , clay pore-volume, clay content, sand pore-volume, and effective porosity

Variable	Mean $\bar{a}$	SD of $a$	$K^*$ ( $\text{m s}^{-1}$ )	Remarks
Measured $K_s$	1.000	0.681	$9.8 \times 10^{-6}$	Total samples
Measured $K_s$	0.999	0.658	$1.1 \times 10^{-5}$	< 10% gravel
Clay pore-volume	1.002	0.363	$7.2 \times 10^{-6}$	Total samples
Clay pore-volume	1.002	0.429	$8.6 \times 10^{-6}$	< 10% gravel
Clay content	1.002	0.441	$8.7 \times 10^{-6}$	< 10% gravel
Sand pore-volume	0.999	0.280	$6.4 \times 10^{-6}$	Total samples
Sand pore-volume	1.000	0.316	$8.0 \times 10^{-6}$	< 10% gravel
Effective porosity	1.000	0.202	$6.2 \times 10^{-6}$	Total samples

pore-volume and sand pore-volume using the specified bulk densities. Comparison of Table 2 with Figs 3 and 4 clearly shows that the assumption of using the bulk density of the fine soil to represent that of the textural elements is justified.

Several factors might have contributed to the variability in  $K_s$  values. Because carved soil monoliths were used, the error due to sample disturbance was negligible. Even though the preceding analysis showed that gravel content contributed in part to the variability in  $K_s$  values, other sources of variability may have come from worm holes, ant holes, and root channels, which were abundant in the topsoil. Prominent large pores due to worms, ants or roots created preferred pathways. Therefore, samples with such features were discarded. However, it was possible that small pores created by tiny worms may not have been detected in some samples.

These findings highlight the common notion that soil texture *per se* is not an attribute of soil structure, but the arrangement of the textural elements with the corresponding pore spaces determines soil structure, which has a remarkable influence on hydraulic conductivity. Within the limits of field spatial variability and experimental errors, the preceding analyses suggest that  $K_s$  of the Alfisol can be predicted within reasonable accuracy from clay or sand pore-volume and effective porosity.

#### (a) Scaled mean saturated hydraulic conductivity

The scaled mean saturated hydraulic conductivity values  $K^*$  calculated using Equation (2) on measured  $K_s$ , and  $K_s$  predicted from clay pore-volume, clay content, sand pore-volume, and effective porosity are given in Table 3. The  $K^*$  values obtained on measured  $K_s$  using all the 109 samples and the non-gravelly soil samples were almost the same and could be approximated as  $1.0 \times 10^{-5} \text{ m s}^{-1}$ . The predicted  $K^*$  values using clay pore-volume, sand pore-volume and effective porosity for all the 109 samples were 72%, 64% and 62% of the measured values, respectively. The  $K^*$  values predicted

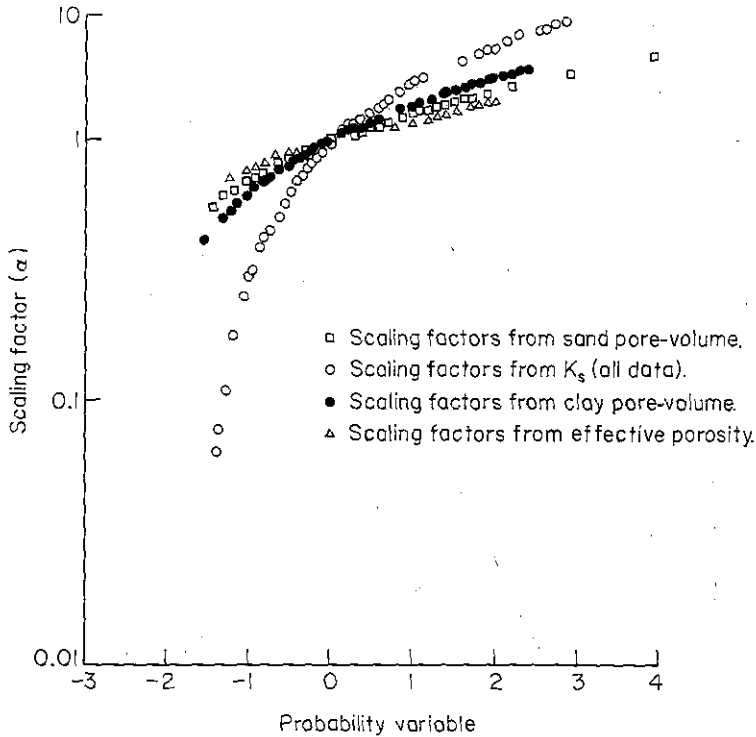


Fig. 6. Semi-log plot of the scaling factors  $\alpha$  derived from sand pore-volume, measured  $K_s$ , clay pore-volume and effective porosity (all data) against the probability variable.

from clay content, clay pore-volume, and sand pore volume for the non-gravelly samples were 87%, 86% and 80%, respectively, of the measured value. It is evident from these results that discounting gravel in the samples improves significantly the predicted values of  $K^*$  from clay content, clay pore-volume and sand pore-volume.

#### (b) Scaling factors

Scaling factors  $a$  obtained from measured  $K_s$ , and  $K_s$  predicted from clay pore-volume, clay content, sand pore-volume, and effective porosity using Equation (4) are also given in Table 3. Considering both the measured and the predicted values together, the mean scaling factors ranged between 0.999 and 1.002, thus agreeing closely with the assumption used in deriving the scaling factor theory (Warrick *et al.*, 1977) that the mean  $a$  value is 1.0. The standard deviation of the scaling factors was highest when the scaling factors were obtained from measured  $K_s$  values, indicating the extent of variability associated with the measured  $K_s$  data.

Fractile diagrams were used to compare the distribution of the scaling factors. These were obtained from the semi-log plots of the scaling factors  $a$  against the probability variable defined as  $(a - \bar{a})/\sigma_a$  (Hald, 1952; Ahuja *et al.*, 1984a), where  $\bar{a}$  is the mean scaling factor, and  $\sigma_a$  is the standard deviation of  $a$ . Fig. 6 shows the fractile diagrams for the scaling factors obtained from measured  $K_s$ , clay pore-volume, sand pore-volume, and effective porosity for all the 109 samples. The distribution of the scaling factors obtained from clay pore-volume, sand pore-volume, and effective porosity was quite similar, but different from that of measured  $K_s$ . The fractile diagrams for the distribution of scaling factors obtained from measured  $K_s$ , clay pore-volume, and clay content for samples containing less than 10% gravel (Fig. 7) shows that the distribution of the scaling factors from clay pore-volume was almost similar to that from clay content and the two distributions almost overlapped. Therefore, we put in only three data points for the clay content to illustrate this.

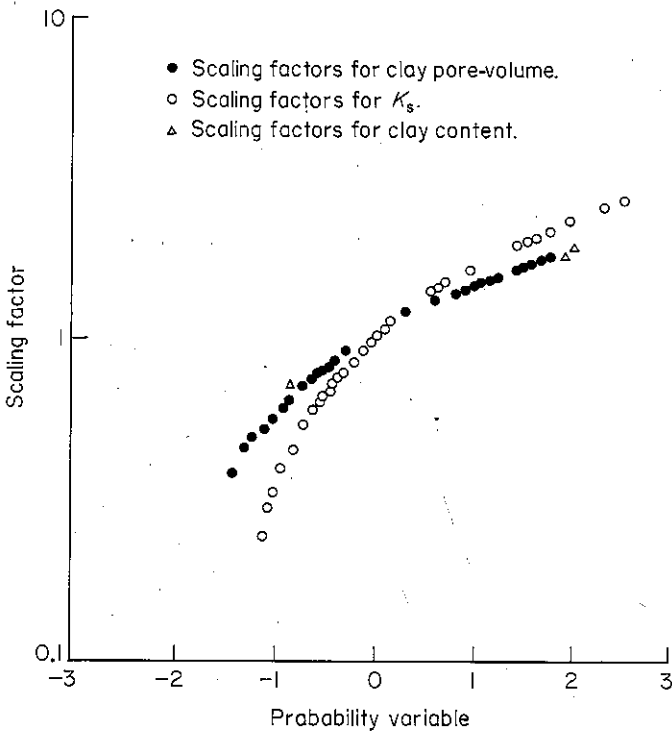


Fig. 7. Semi-log plot of the scaling factors derived from clay pore-volume, measured  $K_s$ , and clay content (samples containing < 10% gravel) against the probability variable.

By discounting the gravelly samples, the distribution of scaling factors obtained from either clay pore-volume or clay content relative to that of measured  $K_s$  improved.

Table 3 and Fig. 7 suggest that  $K_s$  of the Alfisol could be reasonably scaled from clay pore-volume or clay content and sand pore-volume if the gravelly samples are discounted. However, clay pore-volume appears more promising than sand pore-volume because of the higher absolute value of correlation coefficient between  $K_s$  and clay pore-volume. Even though the  $K^*$  obtained from clay content could reasonably approximate that obtained from measured  $K_s$  when the gravelly samples are discounted, the distribution of the scaling factors derived from clay content was discontinuous, reflecting the two textural groups previously discussed. We infer from this study that successful scaling of  $K_s$  from particle size or pore-volume associated with particle size is seriously confounded by the gravel content of the Alfisol. A need for physically based models to resolve this problem of spatial variability in hydraulic properties of gravelly soils is long overdue.

### CONCLUSIONS

This study shows that predicting  $K_s$  of an Alfisol in the SAT using clay pore-volume is confounded by high gravel content. By discounting samples with high gravel content, the success in predicting and scaling  $K_s$  from clay pore-volume becomes remarkable, suggesting a significant contribution of gravel to the variability in  $K_s$  of SAT Alfisols. While the universality of using clay pore-volume to estimate  $K_s$  of SAT Alfisols requires further evaluation, an urgent need for physically based models to address the problem of spatial variability of gravelly Alfisols cannot be over-emphasized.

### ACKNOWLEDGEMENTS

We acknowledge the assistance offered by Mr T. Somaiah in sampling and hydraulic conductivity determination, and by Mr M. Machari Babu for the cartographic assistance. The help we received

from Messrs A. Anjaiah and M. Vidyadhar in particle-size analysis is also acknowledged. We are very grateful to Mr P. N. Murthy for typing the manuscript.

## REFERENCES

- AHUJA, L.R., NANNEY, J.W., GREEN, R.E. & NIELSEN, D.R. 1984a. Macroporosity to characterize spatial variability of hydraulic conductivity and effects of land management. *Soil Science Society of America Journal* **48**, 699-702.
- AHUJA, L.R., NANNEY, J.W. & NIELSEN, D.R. 1984b. Scaling soil water properties and infiltration modeling. *Soil Science Society of America Journal* **48**, 970-973.
- ARYA, L.M. & PARIS, J.F. 1981. A physico-empirical model to predict the soil moisture characteristic from particle-size distribution and bulk density data. *Soil Science Society of America Journal* **45**, 1023-1030.
- BOUMA, J., DEKKER, L.W. & VERLINDEN, H.L. 1976. The vertical hydraulic conductivity at saturation of some Dutch 'Kink' clay soils. *Agricultural Water Management* **1**, 67-70.
- BOUWER, H. & JACKSON, R.D. 1974. Determining soil properties. In *Drainage for Agriculture, Agronomy 17*, (ed. J. van Schifgaarde) pp. 611-672. American Society of Agronomy, Madison, Wisconsin.
- CHILDS, E.C. & COLLIS-GEORGE, N. 1950. The permeability of porous materials. *Proceedings of Royal Society London A* **201**, 392-405.
- CHONG, S.K. & GREEN, R.E. 1979. Application of field-measured sorptivity for simplified infiltration prediction. In *Proceedings of the Hydrologic Transport Modelling*, pp. 88-96. ASAE Publication 4-80, New Orleans, LA, USA.
- EL-SWAIFY, S.A., SINGH, S. & PATHAK, P. 1987. Physical and conservation constraints and management components of SAT Alfisols. In *Alfisols in the Semi-Arid Tropics: A Consultants' Workshop*, pp. 33-48. International Crops Research Institute for the Semi-Arid Tropics (ICRISAT), Patancheru, India.
- HACHUM, A.Y. & ALFARO, J.F. 1977. Water infiltration and runoff under rain application. *Soil Science Society of America Journal* **41**, 960-966.
- HALD, A. 1952. *Statistical theory with engineering applications*. John Wiley and Sons, New York.
- JURY, W.A., RUSSO, D. & SPOSITO, G. 1987. The spatial variability of water and solute transport properties in unsaturated soils. II. Scaling models of water transport. *Hilgardia* **55**, 33-57.
- MARSHALL, T.J. 1958. A relation between permeability and size distribution of pores. *Journal of Soil Science* **9**, 1-8.
- MILLER, E.E. & MILLER, R.D. 1956. Physical theory for capillary flow phenomena. *Journal of Applied Physics* **27**, 324-332.
- PUCKETT, W.E., DANE, J.H. & HAJEK, B.F. 1985. Physical and mineralogical data to determine soil hydraulic properties. *Soil Science Society of America Journal* **49**, 831-836.
- RAVINA, I. & MAGIER, J. 1984. Hydraulic conductivity and water retention of clay soils containing coarse fragments. *Soil Science Society of America Journal* **48**, 736-740.
- SIMMONS, C.S., NIELSEN, D.R. & BIGGAR, J.W. 1979. Scaling of field-measured soil-water properties. I. Methodology. II. Hydraulic conductivity and flux. *Hilgardia* **47**, 77-174.
- TILLOTSON, P.M. & NIELSEN, D.R. 1984. Scale factors in Soil Science. *Soil Science Society of America Journal* **48**, 953-959.
- YOUNGS, E.G. 1987. Estimating hydraulic conductivity values from ring infiltrometer measurements. *Journal of Soil Science* **38**, 623-632.
- WARRICK, A.W., MULLEN, G.J. & NIELSEN, D.R. 1977. Scaling field-measured soil hydraulic properties using a similar media concept. *Water Resources Research* **13**, 355-362.

(Received 28 November 1988; accepted 1 June 1989)